Mitigation of Polarization and Nonlinear Impairments in Optical Fiber using Digital Signal Processing

A Project Report

submitted by

VINOD BAJAJ

in partial fulfilment of the requirements
for the award of the degree of

MASTER OF TECHNOLOGY

DEPARTMENT OF ELECTRICAL ENGINEERING
INDIAN INSTITUTE OF TECHNOLOGY MADRAS.

May 2016

THESIS CERTIFICATE

This is to certify that the thesis titled **Mitigation of Polarization and Nonlinear Impairments in Optical Fiber using Digital Signal Processing**, submitted by **Vinod Bajaj**, to the Indian Institute of Technology, Madras, for the award of the degree of **Master of Technology**, is a bona fide record of the research work done by him under my supervision. The contents of this thesis, in full or in parts, have not been submitted to any other Institute or University for the award of any degree or diploma.

Dr. Deepa Venkitesh
Project Supervisor
Associate Professor
Dept. of Electrical Engineering
IIT-Madras, 600 036

Prof. R. D. Koilpillai
Project Supervisor
Professor
Dept. of Electrical Engineering
IIT-Madras, 600 036

Place: Chennai

Date:

ACKNOWLEDGEMENTS

First and foremost I would like to express my sincere thanks and deepest gratitude to my project supervisors Dr. Deepa Venkitesh and Dr. R. D. Koilpillai, for their inspiring guidance and support. I am sincerely grateful to them for sharing their knowledge and encouraging me through out my research work.

I am thankful to Sterlite Technologies for giving me the opportunity to work on this research. I would also like to thank Prof. Paolo Serena and Optilux team for making open source collection of tools.

I gratefully remember my project group members Smaranika, Lakshmi Narayanan, Sai Bhargav and Siddharth for sharing their knowledge and skills during my work. I really appreciate them for developing other algorithms.

I would like to thank Manas, Amol, Aneesh and LN for always listening to me, and helping me to address the issues related to my work. I cherish the moments spent with LN, Amol, Rohan, Panku and Dattu during my stay at IIT Madras and making this campus feel more like home. I wish to thank Shree, Yusuf, Bhargav, Kavita, Aditi and Guru for sharing light moments during OSA visits, NAVIC launches and Chennai-flood.

I appreciate the awesome support and co-operation from my lab-mates.

Finally, I would like to thank my parents and friends who supported me during every venture of my life.

ABSTRACT

KEYWORDS: Polarization Division Multiplexing, SS-PDM; DBP.

Modern optical communication systems are moving towards spectral efficient system to address the increasing communication traffic. One way to achieve high spectral efficiency is to use Polarization Multiplexing (PM) technique along with higher order modulation format such as QPSK and 16-QAM. Major issue in such system is polarization de-multiplexing in presence of impairments. Moreover advance modulation format needs high OSNR at the receiver for good performance and thus needs high transmission power, but increase in transmitted power induces nonlinear effects and limits the maximum reach of the link.

In this work, we have examined the mitigation techniques for polarization impairments and nonlinear effects through simulations. We have compared the performance of Stokes Space Polarization De-Multiplexing algorithm (SS-PDM) with Constant Modulus Algorithm (CMA). We further demonstrate the effect of nonlinear penalties in a multi-span system. We present results on the mitigation strategies using digital back propagation technique. We demonstrate a better performance of the link by using nonlinearity compensation. Our work concludes with the comparison of experimental data for CMA and SS-PDM for 28 G baud single channel, PM-QPSK and PM-16QAM data. Finally, we demonstrate 32 % increase in maximum reach for PM-QPSK 10.7 G baud system through simulations through nonlinearity compensation. .

TABLE OF CONTENTS

LIST OF TABLES

LIST OF FIGURES

ABBREVIATIONS

IITM	Indian Institute of Technology, Madras
OSNR	Optical Signal to Noise Ratio
QPSK	Quadrature Phase Shift Keying
QAM	Quadrature Amplitude Keying
BER	Bit Error Ratio
EVM	Error Vector Magnitude
DBP	Digital Back Propagation
SS-PDM	Stokes Space Polarization De-Multiplexing
CMA	Constant Modulus Algorithm
RD-CMA	Radially Directed Constant Modulus Algorithm
DSP	Digital Signal Processing
PMD	Polarization Mode Dispersion
SMF	Single Mode Fiber
DGD	Differential Group Delay
SOP	State Of Polarization
PBS	Polarization Beam Splitter
SPM	Self Phase Modulation
XPM	Cross Phase Modulation
PDL	Polarization Dependant Loss
MAP	Maximum A-Priori
VSNE	Volterra Series Nonlinear Equalizer
NLSE	Non-linear Schrodinger Equation
SSFM	Split Step Fourier Method
AWGN	Additive White Gaussian Noise
DD-LMS	Decision Directed Least Mean Square
OMFT	Optical Multi Format Transmitter
PRBS	Pseudo Random Bit Sequence
BP-1S	Back Propagation-1 Span

EDFA	Erbium Doped Fiber Amplifier
FEC	Forward Error Correction

CHAPTER 1

INTRODUCTION

Wireless communication networks are evolving to meet the capacity demand created by multimedia applications. From 2G, 3G, 4G and Long Term Evolution (LTE) 4G, the maximum capacity that must be supported by each mobile cell has progressively increased. Mobile backhaul networks have to handle data rates in the orders of Gbps and beyond. Optical fiber link with Gbps data rate are insufficient overcome the capacity bottleneck of mobile backhauls, need to be updated for supporting higher data rates. The solution to this should comply with the installed resources.

1.1 Coherent Communication - 100 G Standard

Coherent detection has enabled us to use higher order modulation formats, where information can be modulated in both amplitude and phase. Along with this, polarization multiplexing technique can be used to give two fold increment in capacity. These higher order modulation formats are vulnerable to impairments, so DSP equalization is necessary at the receiver. The state of art for 100 Gbps communication system is to use polarization multiplexed 25 G baud QPSK with DSP enabled coherent detection. Figure 1.1 shows block diagram of 100 Gbps communication link, where light from laser source is split into two orthogonal polarizations termed as X and Y using polarization beam splitter (PBS). These two polarizations are externally modulated with data using IQ modulator. After modulation these two polarizations are combined using another PBS and launched into fiber. At receiver end a PBS separates light into two orthogonal polarizations, which are then converted to electrical signal using coherent detection. The electrical signal is then sampled using analog to digital converter (ADC). The transmitted data is then recovered from sampled data after compensation of impairments using digital signal processing (DSP).

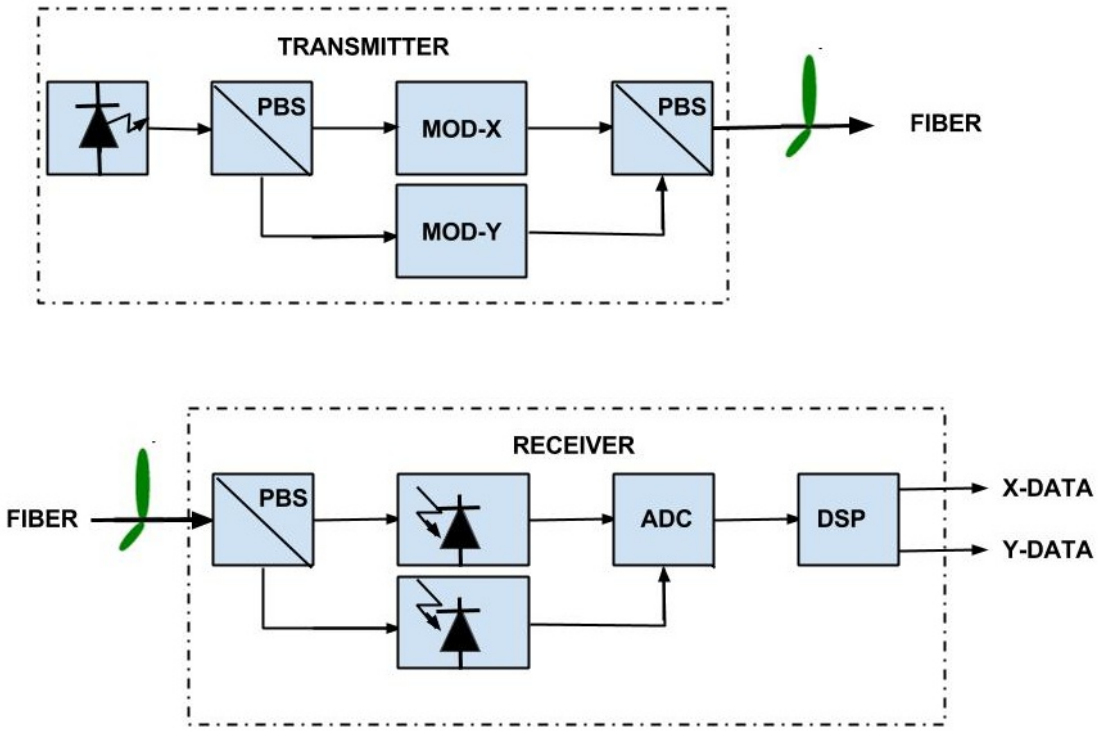

Figure 1.1: Polarization Multiplexed Optical Communication System

1.2 Impairments in Coherent Optical Communication

Based on their origin, impairments in coherent optical communication can be broadly categorized as transmitter - receiver impairments and channel impairments.

Transmitter - receiver impairments are primarily due to laser phase noise and frequency offset. Laser phase noise is due to finite linewidth of laser which adds random phase in signal. Frequency offset is finite detuning between the center frequencies of source and receiver laser, which causes phase addition in signal. These impairments becomes severe when information is modulated in phase as in higher order modulation format, thus need to be compensated at receiver end.

Channel impairments are mainly: Chromatic Dispersion (CD), Polarization Mode Dispersion (PMD) and Kerr nonlinearity. CD occurs because of difference in group velocities of spectral components of signal. It originates because of the material and waveguiding property of fiber, which causes broadening of pulse after propagation through optical fiber. Standard algorithms are already developed by our group to mitigate laser phase noise, frequency offset and chromatic dispersion compensation. In this thesis, we address the polarization impairments and Kerr nonlinearity which are discussed in details.

1.2.1 Polarization Impairments

A Single Mode Fiber (SMF) allows two orthogonal polarizations to propagate with same propagation characteristics. Imperfection in fiber because of the geometry or induced stress due to environmental factors (mechanical stress, temperature variation), introduces birefringence in fiber. Because of the birefringence, the group velocity of the signal depends on the axis along which it is polarized. Let us consider a fiber with

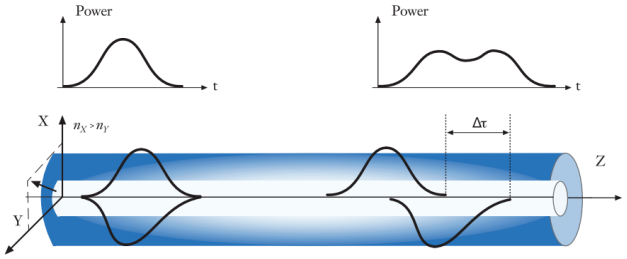

Figure 1.2: PMD

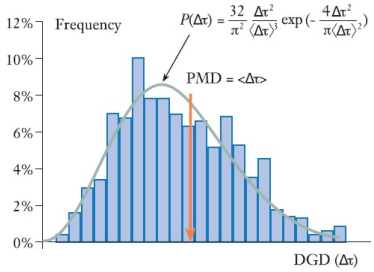

Figure 1.3: DGD Distribution

different refractive index along orthogonal directions ($n_X > n_Y$) (see Figure 1.2). A optical pulse launched into fiber can be resolved into two orthogonal components X and Y. Clearly Y component of the field will travel faster than the X component, resulting in a pulse spread $\Delta\tau$ after propagation, which is called Differential Group Delay (DGD). Fiber can be considered as cascade of several birefringent sections, having different orientation as well as amount of refractive index asymmetry. So the DGD will not be a constant value. For a given length of fiber, it is empirically found that the DGD follows Maxwellian distribution (Figure 1.3). Average of DGD ($< \Delta\tau >$) is termed as Polarization Mode Dispersion (PMD) of fiber. PMD of the fiber is proportional to the square root of length of fiber and the proportionality constant is PMD coefficient PMD_c.

$$PMD \propto \sqrt{L} \Rightarrow PMD = PMD_c\sqrt{L} \tag{1.1}$$

In polarization multiplexed system , SOP of the signal rotates due to fiber birefringence. So the polarization beam splitter (PBS) at receiver end, does not give two independent signals, but a linear combination instead (see Figure 1.4). This phenomenon is called as Polarization Mixing. The presence of other polarization acts as noise in first polarization. So in order to successfully demodulate the signal, these polarizations must be separated.

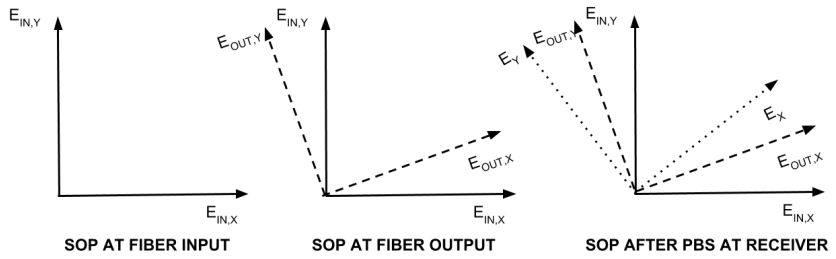

Figure 1.4: Polarization Mixing

1.2.2 Kerr Nonlinearity

Kerr Nonlinearity causes the refractive index of fiber to vary with square of instantaneous electric field intensity

$$\tilde{n}(\omega, |E|^2) = n(\omega) + n_2|E|^2 \tag{1.2}$$

where n_2 is nonlinear refractive index related to third order susceptibility $\chi^{(3)}$.
The change refractive index causes nonlinear phase modulation which can be categorized as Self Phase Modulation(SPM) and Cross Phase Modulation(XPM). SPM is self induced nonlinear phase modulation in optical field during propagation. The phase of optical field is

$$\phi = \tilde{n}k_0L = (n + n_2|E|^2)k_0L \tag{1.3}$$

where $k_0 = \frac{2\pi}{\lambda}$, is free space propagation constant, L is fiber length. The nonlinear phase shift because of SPM is ϕ_{NL} given as

$$\phi_{NL} = n_2|E|^2k_0L \tag{1.4}$$

XPM is nonlinear phase shift in optical field because of optical field at different state of polarization, wavelength or direction (Agrawal (2007)).

1.3 Literature Review

Different DSP based approaches have been proposed for polarization de-multiplexing, which are Kalman filter polarization state tracking, Constant Modulus Algorithm (CMA),

Stokes space polarization de-multiplexing (SS-PDM). Kalman filter based algorithm and CMA are recursive algorithm and its convergence depends on SOP of received signal and hence on initialization parameters value (Chagnon *et al.* (2012); Szafraniec *et al.* (2010); Marshall *et al.* (2010)). CMA is most popular algorithm used for polarization de-multiplexing. CMA with multiple taps can compensate polarization mode dispersion (PMD). Convergence time of CMA can be reduced by using training symbols but it will increase overhead and will need synchronization. Also CMA is related to modulation format and hence, need to be changed if the modulation format changes. Thus CMA is not suitable for adaptive optical packet network, burst mode coherent receivers and agile network architectures. SS-PDM converges fast and can work in the presence of residual carrier frequency, for any square M-QAM modulation format (Chagnon *et al.* (2012)). SS-PDM algorithm can tolerate polarization dependent loss (PDL). Muga and Pinto (2013) have demonstrated performance improvement in SS-PDM by digital PDL compensation. Polarization mode dispersion degrades performance of SS-PDM. A modified method is proposed, in which multi-tap CMA is initialized with SS-PDM. This modified algorithm has improved convergence speed, PDL tolerance, also it can compensate PMD (Yu *et al.* (2013)). Muga and Pinto (2014) have proposed adaptive SS-PDM technique free of best fitting plane thus less complexity in computation.

Large bandwidth-distance product has been achieved using advance modulation formats by full compensation of linear fiber impairments using digital equalization algorithms. The performance of long haul link is limited by nonlinear impairments. Different DSP algorithms have been demonstrated to compensate nonlinear impairments includes maximum a posteriori (MAP) detector, maximum likelihood sequence estimator or Viterbi decoder, transmitter-based electronic precompensation, Volterra series nonlinear equalizer (VSNE), receiver-based electronic phase rotation, extreme learning machine and digital back propagation (Napoli *et al.* (2014); Shen and Lau (2011)). Viterbi decoder and MAP detector based compensation have extremely high complexity for channel with memory and higher order modulation formats. VNSE is also limited by computation complexity. Precompensation algorithm needs high speed DAC along with prior knowledge of link (Millar (2011)). Digital Back Propagation (DBP) was proposed as a universal technique for jointly compensating linear and nonlinear impairment. It exploits physical behavior of channel and propagates signal to inverse channel digitally (Ip and Kahn (2008)). Manakov equations were proposed instead of coupled

polarization nonlinear Schrodinger equation (CP-NLSE) to reduce the computational complexity. These equations were valid because of SOP rotation due to birefringence. DBP involve switching between time and frequency domain, which make it computationally complex. So the research have been focused to reduce the complexity. Rafique *et al.* (2011) have exploited the correlation of signal power between neighboring symbols to reduce number of steps required for DBP. Zhu and Li (2012) proposed dispersion folded DBP for dispersion managed link. Recent work by Guiomar *et al.* (2015) have demonstrated simplified VSNE which is more efficient than DBP. Weighted VSNE is proposed recently by Amado *et al.* (2015) and compared with weighted-SSFM. 80% complexity reduction compared to standard SSFM using weighted-SSFM. Nonlinearity compensation is still an active research topic.

1.4 Objectives

- Implement the Stokes space polarization de-multiplexing algorithm and compare the performance with CMA algorithm.
- Implement Digital Back Propagation (DBP) algorithm and compensate for self phase modulation and cross phase modulation.

1.5 Organization of Report

In this project work, we have considered two problem statements, polarization de-multiplexing and fiber nonlinearity compensation. In chapter 2, CMA and SS-PDM algorithm is discussed and simulation results are compared. Chapter 3 includes experimental implementation of SS-PDM algorithm on 28 G baud data for PM-QPSK and PM-16QAM, and comparison of experimental results. Digital back propagation is discussed in chapter 4. Finally, we conclude our work with scope of future work in chapter 5.

CHAPTER 2

POLARIZATION DE-MULTIPLEXING ALGORITHMS

In this chapter we will discuss constant modulus algorithm and Stokes space polarization de-multiplexing algorithm. The performance of these algorithms is compared for impairments such as birefringence and polarization mixing in simulation environment using MATLAB.

Polarization impaired signal is generated using Jones matrix as shown in following equation Kikuchi (2008)

$$\begin{bmatrix} E_{x,out} \\ E_{y,out} \end{bmatrix} = \begin{bmatrix} \sqrt{\alpha_p}e^{i\delta} & -\sqrt{1-\alpha_p} \\ \sqrt{1-\alpha_p} & \sqrt{\alpha_p}e^{-i\delta} \end{bmatrix} \times \begin{bmatrix} E_{x,in} \\ E_{y,in} \end{bmatrix}$$

where, $E_{x,in}$ and $E_{y,in}$ represent the electric field in two orthogonal polarizations at the input of the fiber; $E_{x,out}$ and $E_{y,out}$ are the respective fields at the output of the fiber, α_p is power splitting ratio and δ is phase delay between the x and y polarizations. Here it is assumed that polarization dependent loss (PDL) is zero, and Jones matrix is frequency independent.

The polarization de-multiplexing algorithm aims to estimate the inverse of the above Jones matrix 'M^{-1}'. This inverse matrix when multiplied with the received signal vector gives de-multiplexed orthogonal polarizations $E_{x,dsp}$ and $E_{y,dsp}$.

$$\begin{bmatrix} E_{x,dsp} \\ E_{y,dsp} \end{bmatrix} = \begin{bmatrix} \sqrt{\alpha_p}e^{-i\delta} & \sqrt{1-\alpha_p} \\ -\sqrt{1-\alpha_p} & \sqrt{\alpha_p}e^{i\delta} \end{bmatrix} \times \begin{bmatrix} E_{x,out} \\ E_{y,out} \end{bmatrix}$$

2.1 Constant Modulus Algorithm

Constant Modulus Algorithm (CMA) is a conventional algorithm used for polarization de-multiplexing. Ideally, for QPSK modulation format, symbols should lie on a circle

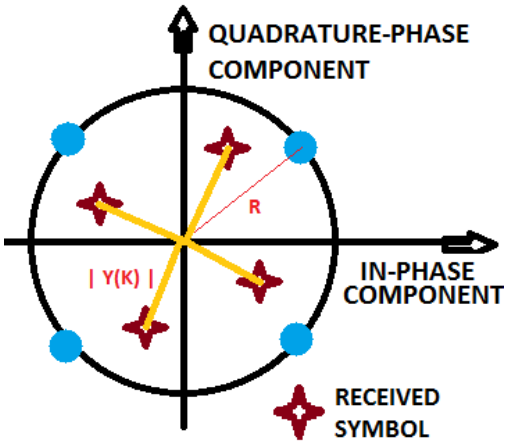

Figure 2.1: CMA

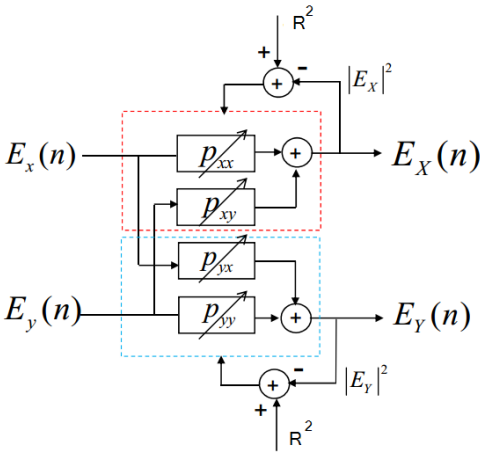

Figure 2.2: Butterfly structure

of constant radius 'R' as shown in Figure 2.1. Polarization mixing deviates the received symbols from the constant circle. CMA uses a DSP butterfly structure (shown in Figure 2.2) to adaptively estimate the inverse Jones matrix so that the symbols are forced to circle of radius 'R' (Kikuchi (2011)). The butterfly structure need to be initialized with tap weights p_{xx}, p_{xy}, p_{yx} and p_{yy}, which are the elements of the inverse Jones matrix. These tap weights are iteratively updated by calculating error for each processed output. If $y(k) = x(k)w(k)$ represent the processed symbol then error is given by

$$e_{CMA} = |y(k)|^2 - R^2,$$

where $x(k)$ and $w(k)$ represent the input symbol and tap weights.
The tap weights are updated using following stochastic gradient update equation:

$$w(k+1) = w(k) - \mu.(e_{CMA}).y(k).x(k)^*$$

where μ is the step size.
Initialization of equalizer and selection of step size is crucial in CMA. Improper tap weights and step size can results in failure of the algorithm. From the above discussion we can see that CMA will work only for constant modulus modulation format. This algorithm need to be modified for modulation format such as 16-QAM. The modified algorithm is known as Radially Directed CMA(RD-CMA). In 16-QAM modulation, the symbols lie on circles of three different radii. So in RD-CMA, each received symbol need to be compared with three different radii. Thus again threshold radii need to be set

appropriately, which might be erroneous in presence of noise and other impairments.

2.2 Stokes Space Polarization Demultiplexing Algorithm

SS-PDM algorithm consists of converting received waveforms into three dimensional Stokes space and then estimating the inverse Jones matrix 'M^{-1}'. Before discussing the algorithm we first discuss in detail, about the Stokes space.

Stokes space is a way to represent polarization of light in 3D sphere, known as Poincare sphere (Figure 2.3[1]). Let the received horizontal and vertical optical signals that emerge from the receiver's polarization beam splitter are e_x and e_y , respectively. The Jones vector that represents of the received optical signal is given as

$$E = \frac{1}{\sqrt{2}} \begin{bmatrix} e_x \\ e_y \end{bmatrix} = \frac{1}{\sqrt{2}} \begin{bmatrix} a_x e^{j(\omega t + \phi_x)} \\ a_y e^{j(\omega t + \phi_y)} \end{bmatrix}$$

where a_x and a_y are the amplitudes and ϕ_x and ϕ_y are the phases of the Jones vector.

The Jones vector representation in above equation can be transformed into Stokes

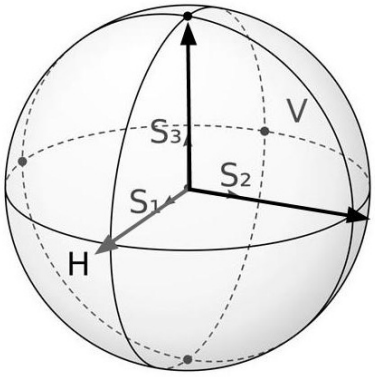

Figure 2.3: Poincare sphere

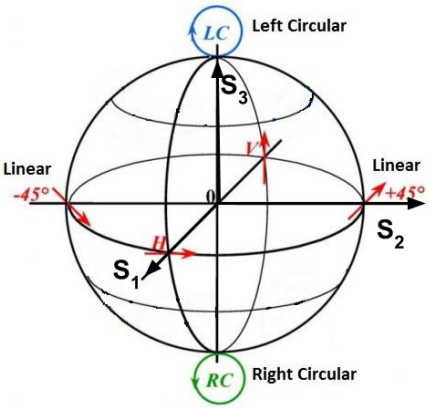

Figure 2.4: Polarization in Stokes space

vectors representation using following relation (Yariv and Yeh (2006))

$$S = \begin{bmatrix} S_0 \\ S_1 \\ S_2 \\ S_3 \end{bmatrix} = \frac{1}{2} \begin{bmatrix} a_x^2 + a_y^2 \\ a_x^2 - a_y^2 \\ 2a_x a_y cos\Delta\phi \\ 2a_x a_y sin\Delta\phi \end{bmatrix}$$

[1] $commons.wikimedia.org/wiki/File : Poincare - sphere_arrows.svg$

where $\Delta\phi = \phi_y - \phi_x$

The first component of the Stokes vector, S_0 , represents total power, and remaining components $[S_1 S_2 S_3]^T$ represent 0^0 linear , 45^0 linear and circularly polarized light respectively (Figure 2.4[2]). Polarization state is visualized in three dimensional space using $[S_1 S_2 S_3]^T$ vector.

Polarization	**Stokes vectors** $[\mathbf{S_1 S_2 S_3}]^{\mathbf{T}}$
Linear 0^0	$[\ 1\ \ 0\ \ 0]^T$
Linear 90^0	$[-1\ \ 0\ \ 0]^T$
Linear 45^0	$[\ 0\ \ 1\ \ 0]^T$
Left circular	$[\ 0\ \ 0\ \ 1]^T$
Right circular	$[\ 0\ \ 0 - 1]^T$

Table 2.1: Stokes vectors for different polarizations

Table 2.2 shows all possible normalized Stokes vector for PM-QPSK. PM-QPSK modulation format get mapped into four states in Stokes space (see Figure 2.5). Here we see that this four states lie in plane $S_1 = 0$.

Figure 2.6 shows transitions between symbols. In complex plane (constellation di-

X	**Y**	$\Delta\phi$	**Stokes vectors**
1 1	1 1	0^0	$[1\ \ 0\ \ 1\ \ 0]^T$
1 1	0 1	90^0	$[1\ \ 0\ \ 0\ \ 1]^T$
1 1	1 0	-90^0	$[1\ \ 0\ \ 0 - 1]^T$
1 1	0 0	180^0	$[1\ \ 0 - 1\ \ 0]^T$

Table 2.2: PM-QPSK Stokes vectors

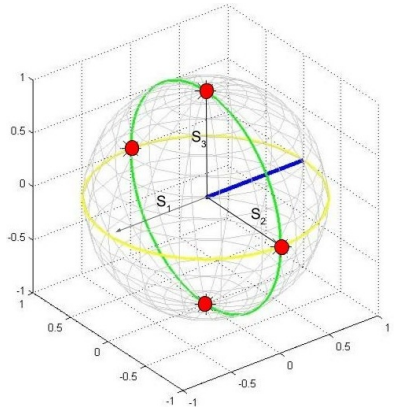

Figure 2.5: PM-QPSK

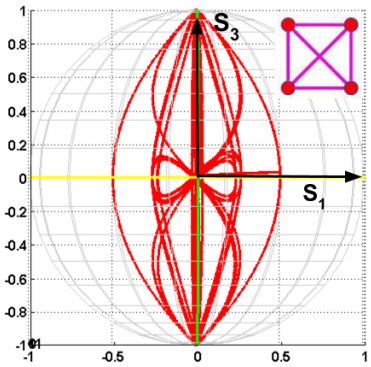

Figure 2.6: PM-QPSK with transitions

[2] Basic Concepts in RADAR Polarimetry:Martin BOERNER

agram) these transitions were linear and simple, but in Stokes space it takes complex trajectory path. These transitions outline lens like object. The lens like object defines a plane and we can see that normal of this plane contains linear horizontal and linear vertical states. So it is the normal that identifies polarization states of transmission.

This lens like structure is formed by any arbitrary modulation format which can be understood through following discussion. Lets consider a hypothetical modulation confined to unit circle in complex plane. This modulation format incorporate all possible modulation scenarios with boundation of unit circle. To make it simple lets fix e_x as 1 and e_y can take any complex value within unit circle. The Jones vector that represents this optical field is:

$$E = \frac{1}{\sqrt{2}} \begin{bmatrix} e_x \\ e_y \end{bmatrix} = \frac{1}{\sqrt{2}} \begin{bmatrix} 1 \\ re^{j\phi} \end{bmatrix}$$

where $0 <= r <= 1$ and $0 <= \phi <= 2\pi$. The corresponding Stokes vector will be

$$S = \begin{bmatrix} S_0 \\ S_1 \\ S_2 \\ S_3 \end{bmatrix} = \frac{1}{2} \begin{bmatrix} 1 + r^2 \\ 1 - r^2 \\ 2rcos\phi \\ 2rsin\phi \end{bmatrix}$$

These set of Stokes vector forms a paraboloidal surface in Stokes space (see Figure 2.7). A similar sets of Stokes vector can be generated with fixing e_y as 1 and varying e_x, which will form a second paraboloidal surface. If both of optical waves take complex value less than 1 then corresponding point will lie in lens structure. Thus formation of lens like object is independent of modulation format (Szafraniec *et al.* (2010)).

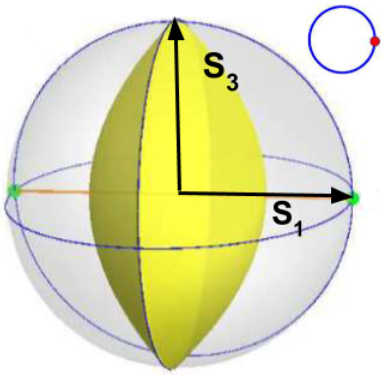

Figure 2.7: Lens formation

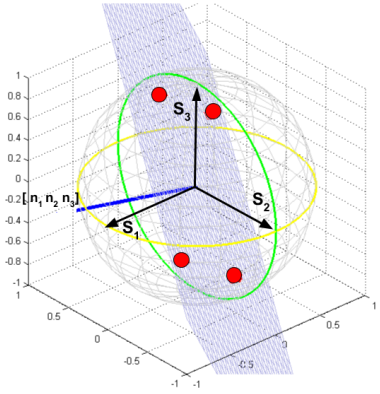

Figure 2.8: Polarization in Stokes space

Fiber birefringence defines an axis in Stokes space, this axis is defined by the eigen-states of polarization (eigenvectors of the matrix), i.e., polarization states that are maintained within the birefringent medium. All other polarization states evolve over the length of the birefringent medium along arcs whose angular measures correspond to the value of the birefringence and whose center is the birefringence axis. Clearly the shape of the disk is preserved in such medium as all its points are rotated around the same axis by the same angle (Szafraniec *et al.* (2010)). PM-QPSK modulation format gets mapped into $S_1 = 0$ plane (Figure 2.5), due to fiber birefringence and polarization mixing effect this plane rotates in 3-D space. Figure 2.8 shows rotated PM-QPSK modulation format in Stokes space. The idea of de-multiplexing the polarization is equivalent to rotating this plane back to $S_1 = 0$ in Stokes space.

2.2.1 Algorithm steps

The received complex symbols are processed in following sequence for polarization de-multiplexing:

- Set power threshold to select outermost constellation symbols, generate Stokes vectors for these symbols.
- Estimate best fit plane containing the Stokes vectors, let say normal to the best fit plane is $[n_1\, n_2\, n_3]$.
- Then the inverse matrix M^{-1} is given by (Chagnon *et al.* (2012))

$$M^{-1} = \begin{bmatrix} cos\,(\theta/2)\, e^{i\Delta\phi/2} & sin\,(\theta/2)\, e^{-i\Delta\phi/2} \\ -sin\,(\theta/2)\, e^{i\Delta\phi/2} & cos\,(\theta/2)\, e^{-i\Delta\phi/2} \end{bmatrix}$$

  where

$$\theta = arc\,tan\left[\frac{\sqrt{n_2^2+n_3^2}}{n_1}\right] \;\; and \;\; \Delta\phi = arc\,tan\left[\frac{n_3}{n_2}\right]$$

- The transmitted horizontal and vertical optical signals are finally obtained by the following transformation

$$\begin{bmatrix} e_h \\ e_v \end{bmatrix} = M^{-1} \begin{bmatrix} e_x \\ e_y \end{bmatrix}$$

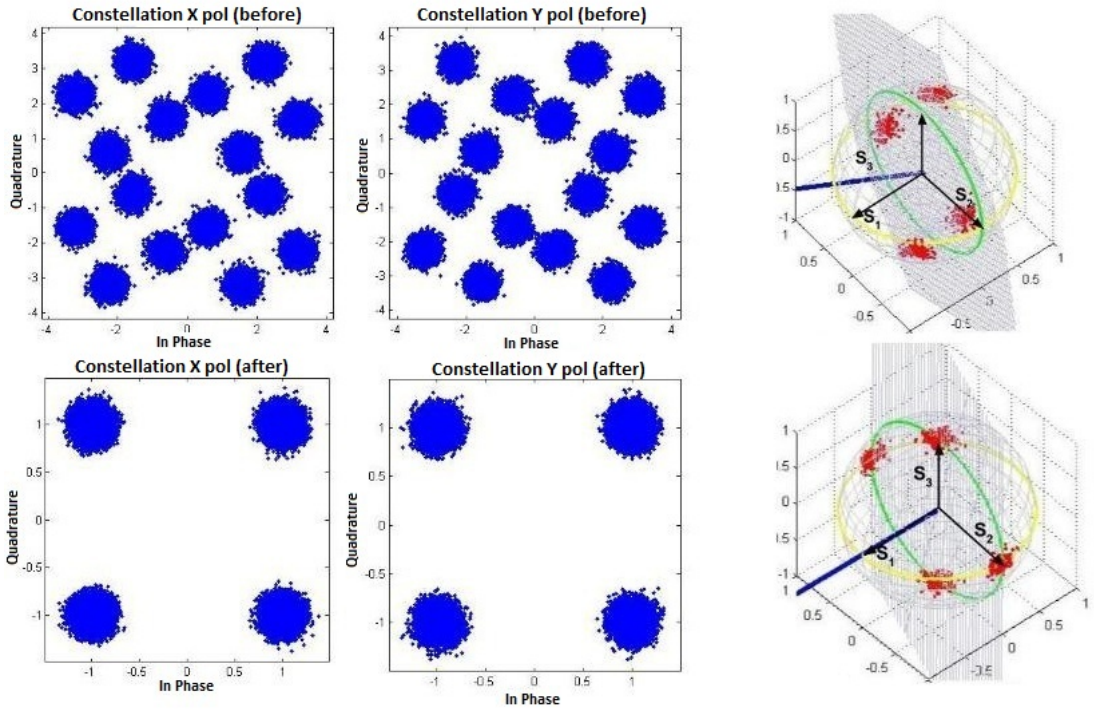

Figure 2.9: PM-QPSK before and after SS-PDM

2.3 Simulation Model

Simulation have been carried out in MATLAB. A PRBS sequence of 2^{16} length is transmitted at 25 G baud rate. Impairments such as laser phase noise and frequency offset were generated using Optilux codes [3]. The transmitter and receiver laser linewidth is taken as 500 KHz with frequency detuning of 1 GHz. Additive White Gaussian Noise (AWGN) is added to maintain OSNR. Polarization impairments were generated using Jones matrix as explained in beginning of chapter. Frequency offset is compensated by using Periodogram technique. Decision Directed Least Mean Square (DD-LMS) algorithm is used for laser phase noise compensation. Polarization impairments are compensated by using either CMA or SS-PDM. Figure 2.9 shows constellation diagram for PM-QPSK before and after processing with SS-PDM at 20 dB OSNR. Here linewidth and frequency offset is set to zero for better visualization.

[3] http://optilux.sourceforge.net/

2.3.1 Simulation Results

BER vs OSNR performance for PM-QPSK and PM16-QAM modulation format is compared in Figure 2.10. We can see that the performance of SS-PDM algorithm is comparable to CMA. For these simulations linewidth and frequency offset is taken as 500 KHz and 1 GHz respectively.

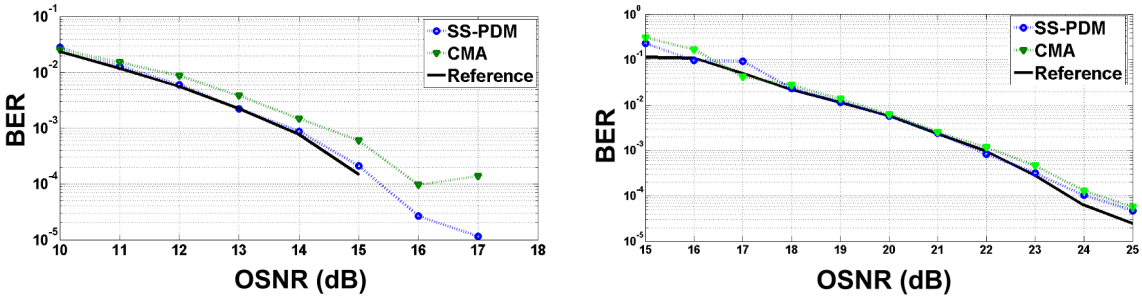

PM-QPSK PM-16QAM

Figure 2.10: BER vs OSNR (back to back)

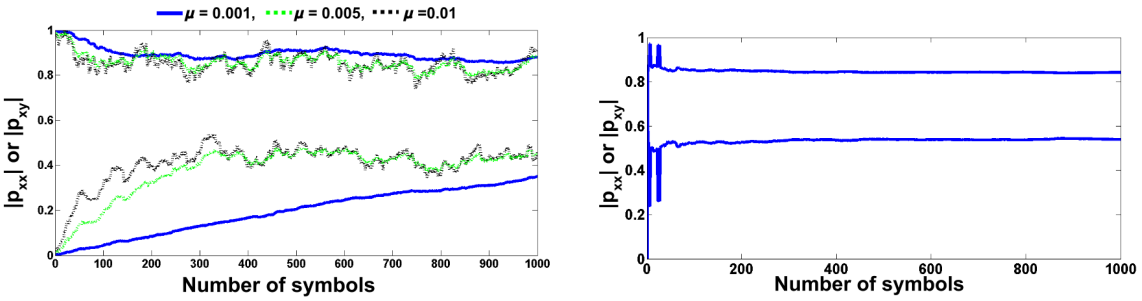

CMA SS-PDM

Figure 2.11: Convergence Plot for PM-QPSK (OSNR 20 dB)

Absolute value of the first row elements of inverse Jones matrix is plotted against number of symbols to analyze speed of convergence of algorithm at 20 dB OSNR. For CMA, convergence plot for PM-QPSK is shown for different step sizes 0.001, 0.005 and 0.01. We can see in Figure 2.11 that CMA with larger step size, leads to faster convergence but converged value have larger fluctuation. It is evident that SS-PDM converges faster than CMA.

2.4 Summary

We can see that SS-PDM is a elegant polarization de-multiplexing technique for burst mode receiver as it converges faster than CMA. Also SS-PDM technique does not have any critical parameter such as initialization of filter tap and step size as in case of CMA. Other aspect is that unlike CMA, SS-PDM is modulation format independent. We have observed that BER vs OSNR performance of SS-PDM is comparable to CMA, also that SS-PDM converges faster then CMA. In the following chapter we will discuss the performance of SS-PDM and CMA through result of post-processing of experimental data.

CHAPTER 3

EXPERIMENTAL RESULTS

The Stokes space polarization de-multiplexing algorithm (SS-PDM) was tested using simulation data in the previous chapter, and we find that SS-PDM has the capability of de-multiplexing the polarization states for any modulation format. We have demonstrated that SS-PDM achieves faster convergence than CMA . So these algorithms are next tested on the experimental data. These experiments were performed in the high speed communication lab at Sterlite Technologies, Aurangabad. In this chapter, we will discuss the experimental setup, the DSP algorithm sequence and results.

3.1 Experimental Setup

The schematic of experimental set up is shown in Figure 3.1. At transmitter side, two sets of 40 narrow linewidth lasers spaced 100 GHz apart are combined by a polarization maintaining (PM) arrayed waveguide grating. This set up produces 80 optical channels with 50 GHz separation covering the entire C band. For our experiment only one of this channel is used. The optical signal from arrayed waveguide grating is fed to an optical multi-format transmitter (OMFT) consisting of a pair of IQ-modulators with polarization multiplexing capability. The OMFT is driven by 4 parallel electrical data channels generated by a 34 G samples/s arbitrary waveform generator (AWG) at the rate of 28 G baud. The modulated signal (a PRBS of length of $2^{31} - 1$ bits) is then pass through a decorrelator. For back to back configuration optical signal from decorrelator is mixed with the noise generated from erbium-doped fiber amplifier(EDFA) and then taken to pre-amplifier at receiver. For optical channel configuration, the signal from optical decorrelator is transmitted over 12 spans, each of length 80 km, of standard G652.D Sterlite OH-LITE fibers with an initial launch power of 0 dBm. The loss of each span(17 dB) is compensated with a variable gain EDFA. No dispersion compensation is used in the link. The received signal is amplified and applied to a phase and polarization diverse coherent receiver. This is followed by a 63 G Samples/s Keysight analog to

digital converter (ADC) which captures the in-phase and quadrature-phase data of each polarization in the digital domain.

The experiment has been done for PM-QPSK and PM-16QAM supporting data rate of 112 Gbps and 224 Gbps, each with two different cases:

- PM-QPSK back to back with variation of OSNR
- PM-QPSK with variation of number of spans
- PM-16QAM back to back with variation of OSNR
- PM-16QAM with variation of number of spans

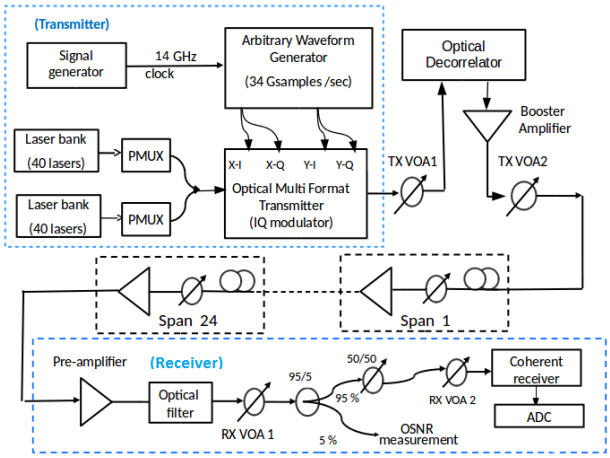

Figure 3.1: Experimental setup

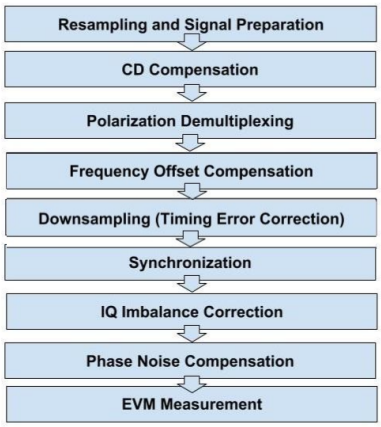

Figure 3.2: DSP algorithm sequence

3.2 Off-line DSP Sequence

The data collected from the ADC is then processed with a sequence of DSP algorithms as shown in Figure 3.2. The data is first re-sampled and pre-processed. The pre-processing step sets mean to zero and normalizes the data. After that CD compensation algorithm is applied. For back to back configuration this step is skipped. Next step is polarization de-multiplexing, which is done with either CMA or SS-PDM. Then after frequency offset is compensated, the signal is down-sampled and synchronized. Thereafter IQ imbalance correction and phase noise compensation is done. Later demodulation is done and performance of the system is evaluated by calculating BER.

3.3 Results

Experimental data is impaired with IQ skew, because of which outer most symbols have difference in magnitude. This will produce unequal number of points for each cluster, So if power threshold is kept high, estimation of inverse Jones matrix will be affected.

In the following results 500 number of symbols were taken for estimation of inverse

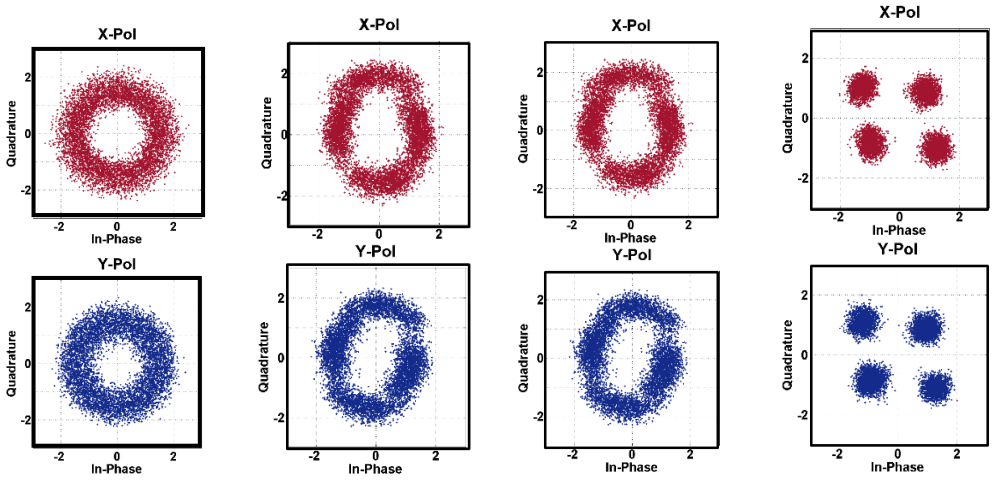

(a) (b) (c) (d)

Figure 3.3: Constellation diagram PM-QPSK processing after (a) SS-PDM (b) Frequency offset compensation (c) IQ imbalance correction (d) Phase noise compensation

Jones matrix. Figure 3.3 shows constellation diagram for PM-QPSK at different stage of processing. BER vs OSNR curve is shown in Figure 3.4 for PM-QPSK and PM-16QAM. Both of the algorithm are performing almost same except some cases where CMA is giving worse BER than SS-PDM. These are the cases where power splitting ratio (α_p) is close to 0.5.

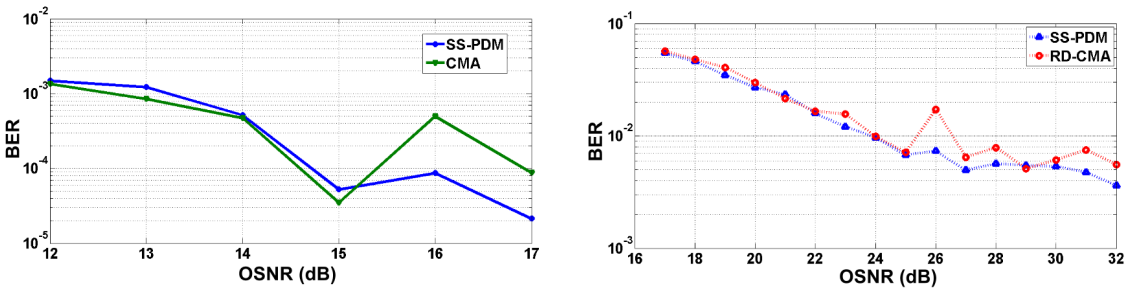

PM-QPSK PM-16QAM

Figure 3.4: BER vs OSNR (back to back)

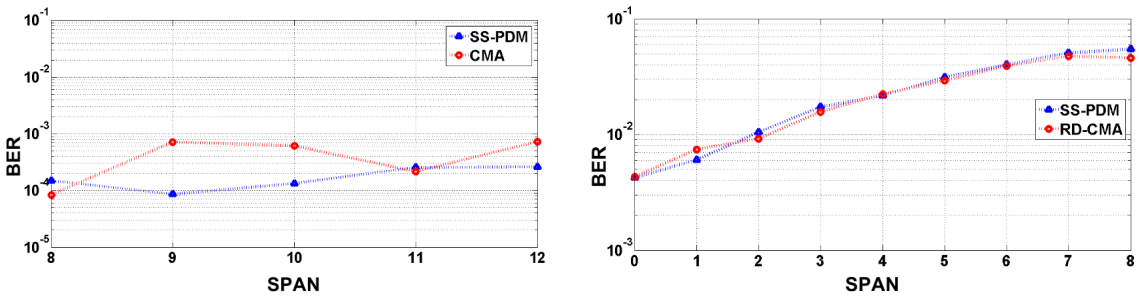

PM-QPSK PM-16QAM

Figure 3.5: BER vs Span

Similarly in BER vs Span plot (see Figure 3.5) for PM-QPSK and PM-16QAM, both algorithm have similar performance. For PM-QPSK we could reach forward error correction (FEC) limit (4.4×10^{-3}). The bias of IQ-modulator drifts over time, which produces un-equispaced constellation.

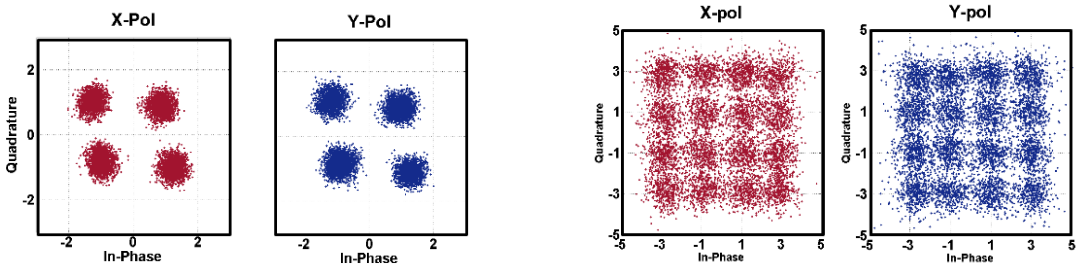

PM-QPSK PM-16QAM

Figure 3.6: Recovered constellation

The effect of IQ modulator drift can be observed in Figure 3.6, which shows recovered constellation after all processing steps. IQ modulator drift effect will be severe for 16-QAM, thus BER for PM-16QAM data did not reach FEC limit.

3.4 Summary

In this chapter we have discussed the processing of 28 G baud experimental data for PM-QPSK and PM-16QAM modulation format. The BER vs OSNR and BER vs Span comparison has been done for both SS-PDM and CMA. The performance of both algorithm is comparable. CMA performance is poorer than SS-PDM in cases of 0.5 power splitting ratio. In the following chapter we will discuss the nonlinearity compensation using Digital Back Propagation.

CHAPTER 4

DIGITAL BACK PROPAGATION

In this chapter we will discuss the field propagation in fiber, nonlinear channel models and algorithm. Self Phase Modulation and Cross Phase Modulation is simulated and compensated using DBP.

4.1 Field Propagation in Fiber

Field propagation in optical fiber can be described through its physical parameters : attenuation constant α, dispersion parameter β_2 and nonlinear coefficient γ. The simplest approximation of propagation of electric field E is provided by Nonlinear Schrodinger Equation Agrawal (2007)

$$\frac{\partial E}{\partial z} = \frac{j\beta_2}{2}\frac{\partial^2 E}{\partial t^2} - j\gamma|E|^2E - \frac{\alpha}{2}E \tag{4.1}$$

where z is propagation axis.

Equation 4.1 models field propagation for single polarization transmission. For polarization multiplexed system, linear and nonlinear interaction of two polarization must have to be considered. Thus the equation 4.1 need to be transformed into vectorized form as:

$$\begin{aligned}\frac{\partial E_X}{\partial z} &= -\frac{\alpha}{2}E_X + \frac{j\beta_2}{2}\frac{\partial^2 E_X}{\partial t^2} - j\gamma\left(|E_X|^2 + \frac{2}{3}|E_Y|^2\right)E_X - \frac{j\gamma}{3}E_X^*E_Y^2 \\ \frac{\partial E_Y}{\partial z} &= -\frac{\alpha}{2}E_Y + \frac{j\beta_2}{2}\frac{\partial^2 E_Y}{\partial t^2} - j\gamma\left(|E_Y|^2 + \frac{2}{3}|E_X|^2\right)E_Y - \frac{j\gamma}{3}E_Y^*E_X^2\end{aligned} \tag{4.2}$$

where E_X and E_Y are orthogonal polarization components of electric field. Since the polarization states of electric field changes rapidly inside fiber due to residual birefringence, the resulting nonlinearity corresponds to an average over entire Poincare sphere (Napoli *et al.* (2014)). This results into Manakov equation. Manakov equations are

more applicable for distances longer than 1000 km.

$$\begin{aligned}\frac{\partial E_X}{\partial z} &= -\frac{\alpha}{2}E_X + \frac{j\beta_2}{2}\frac{\partial^2}{\partial t^2}E_X - j\gamma\frac{8}{9}\left(|E_X|^2 + |E_Y|^2\right)E_X \\ \frac{\partial E_Y}{\partial z} &= -\frac{\alpha}{2}E_Y + \frac{j\beta_2}{2}\frac{\partial^2}{\partial t^2}E_Y - j\gamma\frac{8}{9}\left(|E_X|^2 + |E_Y|^2\right)E_Y\end{aligned} \tag{4.3}$$

4.2 Split Step Fourier Method

The forward propagation equation can be written as (Agrawal (2007)):

$$\frac{\partial \mathbf{E}}{\partial z} = (\hat{N} + \hat{D})\mathbf{E} \tag{4.4}$$

where $\hat{D}$ and $\hat{N}$ are dispersion and nonlinear operator defined as

$$\begin{gathered}\hat{D} = \frac{j\beta_2}{2}\frac{\partial^2}{\partial t^2}, \\ \hat{N} = -\frac{\alpha}{2} - j\gamma\frac{8}{9}\left(\mathbf{E^H E}\right)\mathbf{E}, and \\ \mathbf{E} = \left[E_X \;\; E_Y\right]^T\end{gathered}$$

The solution of equation 4.4 is as follows:

$$E(z+h,t) = e^{h(\hat{D}+\hat{N})}E(z,t) \tag{4.5}$$

where z is current position in span, t is time and h is step size. Above solution can be approximate for sufficiently small step size h by split step fourier method (SSFM) as:

$$e^{h(\hat{D}+\hat{N})}E(z,t) \approx e^{h\hat{D}}e^{h\hat{N}}E(z,t) \tag{4.6}$$

That means each span consists of linear and nonlinear parts cascaded. A common refinement in equation is to evaluate the nonlinear part of the solution with a constant envelope profile and varying intensity. This modification allows larger step sizes to be used as the equation does not imply constant power throughout the step. If it is assumed that over nonlinear part the only change in the electric field is loss, the solution of nonlinear part can be normalized to the varying power profile within the step and the

loss term can be removed (Millar *et al.* (2010)).

$$\begin{aligned}\hat{N}'(\mathbf{E}', z') &= \int_{z}^{z+h} \hat{N}(\mathbf{E}', z')dz' \\ &= \frac{1 - e^{(-\alpha h)}}{\alpha}\hat{N}(\mathbf{E}, z') \\ &= L_{\text{Eff}}\hat{N}(\mathbf{E}, z'), \text{where} \\ \mathbf{E}'(z + h, T) &= e^{(-\alpha h/2)}\mathbf{E}(z, T)\end{aligned} \tag{4.7}$$

The approximation in equation gives us a nonlinear step which includes loss and the total nonlinear phase shift over the spatial step. This is effectively a multiplication by the effective nonlinear length L_{Eff}, given by

$$L_{\text{Eff}} = \frac{1 - e^{(-\alpha h)}}{\alpha} \tag{4.8}$$

Dispersion operator can be applied in two equal parts before and after nonlinear operator to improve accuracy, which results in symmetric SSFM.

$$e^{h(\hat{D}+\hat{N})}E(z, T) \approx e^{\left(\frac{h\hat{D}}{2}\right)}e^{L_{\text{Eff}}\hat{N}}e^{\left(\frac{h\hat{D}}{2}\right)}E\left(z, T\right) \tag{4.9}$$

4.3 Nonlinear Models

Each SSFM method can be described in mainly three different nonlinear models which are: the Wiener model, which is cascade of a linear block followed by a memoryless nonlinear block (Figure 4.1(a)), the Hammerstein model, which consists of a memoryless nonlinear block followed by a linear block (Figure 4.1(b)), and the Wiener - Hammerstein model, which represents the concatenation of the Wiener and Hammerstein models, that is, a linear block followed by a memoryless nonlinear block, followed by a second linear block (Figure 4.1(c)) (Millar *et al.* (2010)). Clearly, the Wiener-Hammerstein model represents symmetric SSFM. These models as cascaded forms complete channel. The Wiener-Hammerstein model gives better accuracy than Wiener model for same step size. Solution of Manakov equation need to be performed at receiver over noisy signal and it should be least complex. Recent research demonstrates that DBP with single nonlinear step per span with bulk step is sufficiently accurate solution of Manakov equation (Millar (2011)).

(a) (b) (c)

Figure 4.1: Nonlinear channel model (a) Wiener (b) Hammerstein (c) Wiener Hammerstein

4.4 Digital Back Propagation Algorithm

The DBPs have two variations - the Wiener model based or the Weiner-Hammerstein model based. We have considered Wiener model. Dispersive and Nonlinear operators are applied in frequency domain and time domain respectively (Millar *et al.* (2010)).

$$\begin{aligned} \exp(h\hat{D})\mathbf{E} &= \mathcal{F}^{-1}\{\exp(h\mathcal{F}\{\hat{D}\})\mathcal{F}\{\mathbf{E}\}\} \\ \hat{N}(t, z_{\mathrm{NL}}) &= j\varphi z_{\mathrm{NL}}(|E_X(t)|^2 + |E_Y(t)|^2)P_L \end{aligned} \tag{4.10}$$

Here P_L is lauch power, z_{NL} is nonlinear step size and ϕ is a constant to be optimized. If step size is smaller than span length then exponentially attenuating power profile need to be considered. So the nonlinear operator modified as

$$\hat{N}(t, z_{\mathrm{NL}}) = j\varphi 10^{(sL/10n)} z_{\mathrm{NL}}(|E_X(t)|^2 + |E_Y(t)|^2)P_L \tag{4.11}$$

where n is number of steps per span, s is step index and L is loss in dB for each span.

4.5 Simulation Model and Results

Simulation model is similar to what is explained in chapter 2 with addition of nonlinear effect SPM and XPM. QPSK signal at 10.7 G baud rate is transmitted with different launch power over a link of 2560 Km (32 span). Simulation parameters are tabulated (see Table 4.1). Transmitter and receiver laser linewidth are 1 MHz and 10 KHz respectively. Local oscillator to signal power ratio is taken as 24 dB. DBP is modeled as the Weiner model. EDFA's are considered to have saturated gain of 17 dB, which is then attenuated to maintain same input power for each span. Average PMD coefficient is considered as $0.1ps/\sqrt{km}$. Nonlinear phase modulation was simulated using SSFM with step size of 10km. Error Vector Magnitude is calculated to estimate BER. Q factor is plotted against launched power for without any nonlinear compensation (NLC)

and with BP-1S (i.e. DBP with step size of 1 span) (see Figure 4.2). We can see that -3 dBm is optimum launch power without NLC, and the Q factor starts decreasing if launch power is increased due to nonlinear effect. Nonlinear phase rotation is compensated by BP-1S with Q factor improvement of 0.73 dB.

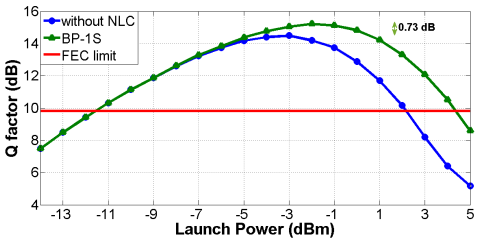

Figure 4.2: Q factor vs launch power

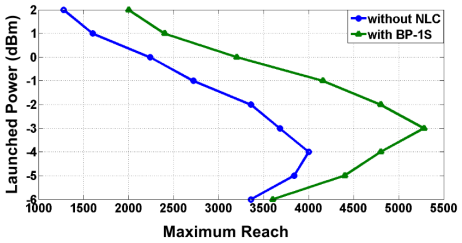

Figure 4.3: Maximum reach of PM-QPSK

Now after plotting Q factor improvement, we can apply BP-1S to increase maximum reach of system. Maximum reach of system is taken as longest length to maintain 10^{-3} BER or equivalently Q factor of 9.8 dB. For this simulation, receiver side ADC resolution is included, which is assumed to be 4 bits. Maximum reach is plotted with

Parameters	**Value**
α[dB/km]	0.19
D[ps/km/nm]	16.87
$\gamma[1//W/km]$	1.2
Span length [km]	80.2
Optical filter bandwidth [GHz]	100
EDFA noise figure [dB]	4.5

Table 4.1: Fiber link parameters

and without NLC in Figure 4.3. Optimum launch power is -4 dBm and longest reach is 4000 Km for case of without NLC. Optimum launch power for BP-1S is -3 dBm with longest reach of 5280 Km. Clearly we see that BP-1S has increased the reach of the link by 32%.

4.6 Summary

DBP is universal technique for joint compensation of linear and nonlinear impairments. It enhances nonlinearity tolerance of system and enables system to perform in low OSNR. QPSK and 16-QAM signal can be transmitted to longer distances using receiver with DSP along with DBP.

CHAPTER 5

CONCLUSION

5.1 Summary of work done

We have done simulations to study the impairments in polarization multiplexed communication systems with higher order modulation format such as QPSK and 16-QAM. We have implemented Stokes space polarization de-multiplexing(SS-PDM) algorithm. A comparative study has been done for SS-PDM algorithm and constant modulus algorithm (CMA). We have compared convergence of both algorithm through simulation. 28 G baud experimental data for PM-QPSK and PM-16QAM were processed with both of the algorithm and comparative results have been produced.

We have studied nonlinear phase modulation in optical fiber due to Kerr nonlinearity. We have simulated the effect of self phase modulation and cross phase modulation. We have implemented Digital Back Propagation algorithm to compensate nonlinear effect in polarization multiplexed system. Simulations have been done to find optimum step size parameter. We have shown that significant improvement can be achieved using DBP. We have improved maximum reach of PM-QPSK 10.7 G baud system by 20%, using digital back propagation. Finally we have discussed realization of DBP.

5.2 Scope for future work

SS-PDM algorithm can be extended for polarization dependent loss compensation. Polarization mode dispersion tolerance can be improved using Kalman filter. SS-PDM can be used to initialize filter tap in multiple tap CMA. Such algorithm can compensate PMD, with fast convergence. Complexity of SS-PDM can be reduced by using geometrical approach, which does not require best plane fitting. Kalman filter based polarization state and carrier tracking algorithm can also be exploited.

A detailed investigation of DBP algorithm need to done to reduce its complexity by

exploiting DSP technique. DBP algorithm can be extended to compensate for cross phase modulation in wavelength division multiplexed (WDM) systems . Volterra series nonlinear equalizer can be implemented in simulations. Nonlinear phase noise (NLPN) should also be addressed using simulations.

APPENDIX A

MATLAB simulation codes

Code for Stokes Space Polarization De-Multiplexing Algorithm

```
function [E_x_dmx,E_y_dmx,M_inv] = stokes_space_v04(
    E_x_mx,E_y_mx,Pth)
% PROGRAM : POLARIZATION DUMULTIPLEXING USING STOKES
    SPACE
% AUTHORS : VINOD BAJAJ

global ideal_IQ_RMS
scale_x = modnorm(E_x_mx,'avpow',ideal_IQ_RMS.^2);      %
    scale down the Rx constellation power
scale_y = modnorm(E_y_mx,'avpow',ideal_IQ_RMS.^2);      %
    to ideal constellation power
E_x_mx = E_x_mx*scale_x;
E_y_mx = E_y_mx*scale_y;
P = abs(E_x_mx).^2+abs(E_y_mx).^2;                      %
    calcualate power
Pnorm = sum(P)/length(P);
P = P/Pnorm;                        % normalized power vector
index = find(P>Pth);                %% Select symbols with
    power > Pth%
n_elmnt = length(index)

RX_x_th = zeros(n_elmnt,1);
RX_y_th = zeros(n_elmnt,1);
for i = 1:n_elmnt
    loc = index(i);
    RX_x_th(i,1) = E_x_mx(loc);
    RX_y_th(i,1) = E_y_mx(loc);
```

```
22 end
23 [ RX_X_angle, RX_X_mag] = cart2pol(real(RX_x_th),imag(
     RX_x_th));
24 [ RX_Y_angle, RX_Y_mag] = cart2pol(real(RX_y_th),imag(
     RX_y_th));
25 d_phi = (RX_Y_angle-RX_X_angle);
26 St = zeros(length(RX_x_th),3);
27 St(:,1) = 0.5*(RX_X_mag.^2-RX_Y_mag.^2);          %
     calculate Stokes vectors
28 St(:,2) = RX_X_mag.*RX_Y_mag.*cos(d_phi);
29 St(:,3) = RX_X_mag.*RX_Y_mag.*sin(d_phi);
30
31 % addpath to fitNormal function
32 figure(1); P_hole = fitNormal(St,1);  % function to
     esimate best fit plane
33 if P_hole(2)<0
34     P_hole = -P_hole;
35 end
36 theta_F  = acos(dot(P_hole,[1 0 0]))*180/pi;
37 ALP  = 0.5*theta_F;
38 PHI  = atan(P_hole(3)/P_hole(2))*180/pi;
39 if PHI<0
40     PHI = 180 + PHI;
41 end
42
43 a_r = ALP *pi/180;
44 p_r = PHI*pi/180;
45 a_c = cos(a_r)*exp(1i*p_r/2);
46 b_c = sin(a_r)*exp(-1i*p_r/2);
47 M_inv = [   a_c          b_c;...                  % inverse
     Jones matrix
48          -conj(b_c)      conj(a_c)];
49 E_dmx = M_inv*[E_x_mx.'; E_y_mx.'];
```

```
50 E_x_dmx = E_dmx(1,:).';                                    %
       demultiplexed polarizations
51 E_y_dmx = E_dmx(2,:).';
52 end
```

Code for estimating best fit plane

```
1  function n = fitNormal(data, show_graph)
2  %FITNORMAL - Fit a plane to the set of Stoke vectors
3
4  %For a passed list of points in (x,y,z) cartesian
       coordinates,
5
6          if nargin == 1
7                  show_graph = false;
8          end
9
10         for i = 1:3
11                 X = data;
12                 X(:,i) = 1;
13
14                 X_m = X' * X;
15                 if det(X_m) == 0
16                         can_solve(i) = 0;
17                         continue
18                 end
19                 can_solve(i) = 1;
20
21                 % Construct and normalize the normal
                       vector
22                 coeff = (X_m)^-1 * X' * data(:,i);
23                 c_neg = -coeff;
24                 c_neg(i) = 1;
```

```
25                  coeff(i) = 1;
26                  n(:,i) = c_neg / norm(coeff);
27
28          end
29
30          if sum(can_solve) == 0
31                  error('Planar fit to the data caused a
                        singular matrix.')
32                  return
33          end
34
35          % Calculating residuals for each fit
36          center = mean(data);
37          off_center = [data(:,1)-center(1) data(:,2)-
                center(2) data(:,3)-center(3)];
38          for i = 1:3
39                  if can_solve(i) == 0
40                          residual_sum(i) = NaN;
41                          continue
42                  end
43
44                  residuals = off_center * n(:,i);
45                  residual_sum(i) = sum(residuals .*
                        residuals);
46
47          end
48
49          % Find the lowest residual index
50          best_fit = find(residual_sum == min(residual_sum)
                );
51
52          % Possible that equal mins so just use the first
                index found
```

```
53          n = n(:,best_fit(1));
54
55          if ~show_graph
56                  return
57          end
58
59          range = max(max(data) - min(data)) / 2;
60          mid_pt = (max(data) - min(data)) / 2 + min(data);
61      xlim = [-1 1];
62          ylim = [-1 1];
63          zlim = [-1 1];
64  %       xlim = [-1 1]*range + mid_pt(1);
65  %       ylim = [-1 1]*range + mid_pt(2);
66  %       zlim = [-1 1]*range + mid_pt(3);
67
68      Pno = sqrt((abs(data(:,1)).^2+abs(data(:,2)).^2+abs(
            data(:,3)).^2));
69
70      data(:,1) = data(:,1)./Pno;
71      data(:,2) = data(:,2)./Pno;
72      data(:,3) = data(:,3)./Pno;
73
74          L=plot3(data(:,1),data(:,2),data(:,3),'r.','
                Markerfacecolor','r'); % Plot the original data
                 points
75          hold on;
76      %% plotting sphere
77      [x,y,z] = sphere(18);
78      M = mesh(x,y,z);
79      set(M,'facealpha',0)
80      set(M,'edgecolor',[.8 .8 .8])
81      tc = linspace(0,2*pi);
82      zc = cos(tc);
```

```
83      yc = sin(tc);
84      xc = 0*tc;
85      hold on;
86      plot3(xc,yc,zc,'g','LineWidth',2); hold on;
87      plot3(zc,yc,xc,'y','LineWidth',2)
88      %% plotting plane for normal
89      center = [0 0 0];
90      d = -center*n; %'# dot product for less typing
91      [xx,yy]=meshgrid(-1:.05:1,-1:.05:1);
92  %     %# calculate corresponding z
93      z = (-n(1)*xx - n(2)*yy - d)/n(3);
94      P = surf(xx,yy,z);
95      set(P,'facealpha',0)
96      set(P,'edgecolor',[.7 .7 .9])
97      %%
98
99          set(get(L, 'Parent'),'DataAspectRatio',[1 1 1],'
                XLim',xlim,'YLim',ylim,'ZLim',zlim);
100
101 %         norm_data = [mean(data); mean(data) + (n' * range
    )]
102     origin_ = [0 0 0];
103     norm_data = [origin_; origin_ + (n' * range)];
104     if norm_data(2,2)<0
105         norm_data(2,:) = -norm_data(2,:);
106     end
107         % Plot the original data points
108         L=plot3(norm_data(:,1),norm_data(:,2),norm_data
                (:,3),'b-','LineWidth',3);
109         set(get(get(L,'parent'),'XLabel'),'String','x','
                FontSize',14,'FontWeight','bold')
110         set(get(get(L,'parent'),'YLabel'),'String','y','
                FontSize',14,'FontWeight','bold')
```

```
111             set(get(get(L,'parent'),'ZLabel'),'String','z','
                    FontSize',14,'FontWeight','bold')
112             title(sprintf('Normal Vector: <%0.3f, %0.3f, %0.3
                    f>',n),'FontWeight','bold','FontSize',14)
113             grid on;
114             axis square;
115         xlabel('S_1','FontSize',14,'FontWeight','bold','Color
                ','black');
116         ylabel('S_2','FontSize',14,'FontWeight','bold','Color
                ','black');
117         zlabel('S_3','FontSize',14,'FontWeight','bold','Color
                ','black');
118
119             hold off;
120 end
```

Code for Digital Back Propagation Algorithm

```
1  function  [x,y]= dbp_step3(u,v,Nspan,gam_m,betat,Ptx,n,z,
       phi)
2  %
3  % PROGRAM : COMPENSATION OF SPM and XPM (single channel)
4  % AUTHORS : VINOD BAJAJ
5
6  % Code for BP-n S
7  % Ptx is in mW, each span treated as single step,
8  % z is length 80.2 km
9  % phi needs to be optimized..
10 % dz = step size
11 %  n stands for BP-nS
12 % gam_m = nonlinear parameter in 1/mW/km
13
14 dz = z/n;
```

```
15 alphalin = 4.6052e-05;
16 leff = (1-exp(-alphalin*dz))/alphalin;  % effective
     length
17 Hxx = fastexp(betat*dz);
18 gamleff = gam_m*phi*leff*Ptx;
19      for jk = 1:Nspan*n
20          pow = (real(u).^2 + imag(u).^2)+(real(v).^2 +
               imag(v).^2);
21          phi_nl=pow.*gamleff;
22          u = u.*fastexp(phi_nl);%  Nonlinear compnesation
23          v = v.*fastexp(phi_nl);%
24          ux = fft(u);
25          vx = fft(v);
26          ux = Hxx.*ux;              % Linear compnesation /
               Dispersion compensation
27          vx = Hxx.*vx;
28          u=ifft(ux);
29          v=ifft(vx);
30       end
31 x =  u;                            % compensated data
32 y =  v;
```

REFERENCES

1. **Agrawal, G. P.**, *Nonlinear fiber optics*. Academic press, 2007.

2. **Amado, S. B.**, **F. P. Guiomar**, **N. J. Muga**, **R. M. Ferreira**, **J. D. Reis**, **S. M. Rossi**, **A. Chiuchiarelli**, **J. R. Oliveira**, **A. L. Teixeira**, and **A. N. Pinto** (2015). Low complexity advanced dbp algorithms for ultra-long-haul 400g transmission systems.

3. **Chagnon, M.**, **M. Osman**, **X. Xu**, **Q. Zhuge**, and **D. V. Plant** (2012). Blind, fast and sop independent polarization recovery for square dual polarization–mqam formats and optical coherent receivers. *Optics express*, **20**(25), 27847–27865.

4. **Guiomar, F. P.**, **S. B. Amado**, **A. Carena**, **G. Bosco**, **A. Nespola**, **A. L. Teixeira**, and **A. N. Pinto** (2015). Fully blind linear and nonlinear equalization for 100g pm-64qam optical systems. *Journal of Lightwave Technology*, **33**(7), 1265–1274.

5. **Ip, E.** and **J. M. Kahn** (2008). Compensation of dispersion and nonlinear impairments using digital backpropagation. *Lightwave Technology, Journal of*, **26**(20), 3416–3425.

6. **Kikuchi, K.**, Polarization-demultiplexing algorithm in the digital coherent receiver. *In 2008 Digest of the IEEE/LEOS Summer Topical Meetings*. 2008.

7. **Kikuchi, K.** (2011). Performance analyses of polarization demultiplexing based on constant-modulus algorithm in digital coherent optical receivers. *Optics express*, **19**(10), 9868–9880.

8. **Marshall, T.**, **B. Szafraniec**, and **B. Nebendahl** (2010). Kalman filter carrier and polarization-state tracking. *Optics letters*, **35**(13), 2203–2205.

9. **Millar, D. S.** (2011). *Digital signal processing for coherent optical fibre communications*. Ph.D. thesis, UCL (University College London).

10. **Millar, D. S.**, **S. Makovejs**, **C. Behrens**, **S. Hellerbrand**, **R. I. Killey**, **P. Bayvel**, and **S. J. Savory** (2010). Mitigation of fiber nonlinearity using a digital coherent receiver. *Selected Topics in Quantum Electronics, IEEE Journal of*, **16**(5), 1217–1226.

11. **Muga, N. J.** and **A. N. Pinto** (2013). Digital pdl compensation in 3d stokes space. *Journal of Lightwave Technology*, **31**(13), 2122–2130.

12. **Muga, N. J.** and **A. N. Pinto** (2014). Adaptive 3-d stokes space-based polarization demultiplexing algorithm. *Journal of Lightwave Technology*, **32**(19), 3290–3298.

13. **Napoli, A.**, **Z. Maalej**, **V. A. Sleiffer**, **M. Kuschnerov**, **D. Rafique**, **E. Timmers**, **B. Spinnler**, **T. Rahman**, **L. D. Coelho**, and **N. Hanik** (2014). Reduced complexity digital back-propagation methods for optical communication systems. *Journal of Lightwave Technology*, **32**(7), 1351–1362.

14. **Rafique, D.**, **M. Mussolin**, **M. Forzati**, **J. Mårtensson**, **M. N. Chugtai**, and **A. D. Ellis** (2011). Compensation of intra-channel nonlinear fibre impairments using simplified digital back-propagation algorithm. *Optics express*, **19**(10), 9453–9460.

15. **Shen, T. S. R.** and **A. P. T. Lau**, Fiber nonlinearity compensation using extreme learning machine for dsp-based coherent communication systems. *In 16th Opto-Electronics and Communications Conference*. 2011.

16. **Szafraniec, B.**, **B. Nebendahl**, and **T. Marshall** (2010). Polarization demultiplexing in stokes space. *Optics express*, **18**(17), 17928–17939.

17. **Yariv, A.** and **P. Yeh**, *Photonics: optical electronics in modern communications (the oxford series in electrical and computer engineering)*. Oxford University Press, Inc., 2006.

18. **Yu, Z.**, **X. Yi**, **J. Zhang**, **M. Deng**, **H. Zhang**, and **K. Qiu** (2013). Modified constant modulus algorithm with polarization demultiplexing in stokes space in optical coherent receiver. *Lightwave Technology, Journal of*, **31**(19), 3203–3209.

19. **Zhu, L.** and **G. Li** (2012). Nonlinearity compensation using dispersion-folded digital backward propagation. *Optics express*, **20**(13), 14362–14370.